Research Paper
Journal of Aerospace System Engineering
Vol.14, No.2, pp.20-27 (2020)

EISSN 2508-7150
http://dx.doi.org/10.20910/JASE.2020.14.2.20

Sliding Mode Control for an Intelligent Landing Gear Equipped with Magnetorheological Damper

Luong Quoc Viet[1], Hyo-sang Lee[1], Dae-sung Jang[1] and Jai-hyuk Hwang[1,†]

[1]Dept of Aerospace and mechanical Engineering, Korea Aerospace University

Abstract

Several uncertainties in the landing environment of an aircraft are not considered, such as the falling speed, ambient temperature, and sensor noise. These uncertainties negatively affect the performance of the controller applied to a landing gear. The sliding mode control (SMC) method, which maintains the optimal performance of a controller under uncertainties, is used in this study. The landing gear is equipped with a magnetorheological damper that changes the yield shear stress according to the applied magnetic field. The applied controller employs a hybrid control combining Skyhook control and force control. The SMC maintains the optimal performance of the hybrid control by minimizing the tracking error of the damper force, even in various landing environments where parameter uncertainties are applied. The effect of SMC is verified through co-simulation results from Simscape and Simulink.

Key Words: Uncertainty, Sliding Mode Control, MR Damper, Hybrid Control, Tracking Error, Co-simulation

1. Introduction

An aircraft landing gear must minimize the load on the airframe and the vibration transmitted to passengers by effectively absorbing the impact on the aircraft during landing. Currently, hydraulic and pneumatic manual landing gears are used extensively in aircraft [1]. The manual landing gear offers advantages such as simple structure, low weight, and stability; however, the optimal efficiency can be achieved only under the operation conditions considered during design. The active landing gear was designed in the 1970s to maintain good landing efficiency under various landing situations [2,3]. However, the active landing gear failed to be commercialized because it required a separate power source, which resulted in a complex structure and a heavy weight, and because of its disadvantage where safety cannot be guaranteed when controller failure occurs [4].

The semi-active landing gear investigated recently offers advantages of sustained optimal performance even in various landing situations owing to the applicability of a feedback control method and safety assurance even when the controller is broken, through its passive mode. A semi-active landing gear applied with a magnetorheological (MR) damper was investigated in this study. The MR damper is an intelligent damper that changes the yield shear stress of a fluid according to the magnetic field applied. The MR damper is used in many fields because it can form a shear stress using a small power and affords a fast reaction.

Many semi-active control methods for aircraft landing gears have been studied [5-10]. The maximum compression stroke of a landing gear has been reduced in a study applying the Skyhook control method, which is used in vehicle suspension to aircraft; however, the improvement in the landing impact absorption efficiency is limited [5]. Hence, a hybrid control method combining the Skyhook control method with a load control method has been suggested [6]. However, these methods deteriorate the control performance owing to unconsidered environments and modeling uncertainties. Therefore, many advanced control methods have been investigated to guarantee the control performance in various landing environments. Optimal controls to compensate performance degradation in various falling speeds have been studied [7] as well as intelligent controllers that consider variations in aircraft mass [8]. Furthermore, robust control based on H_∞ has been applied to increase the robustness of landing gears in various landing situations [9]. In addition, the first-order sliding mode control (SMC) method has been applied to reduce aircraft vibration when model uncertainties

Received: Aug. 12, 2019 Revised: Jan. 03, 2020 Accepted: Jan. 07, 2020
† Corresponding Author
Tel: +82-2-300-0109, E-mail: jhhwang@kau.ac.kr

appear [10].

However, existing studies on semi-active landing gear controllers do not consider sensor noise. Sensor noise must be considered because it deteriorates the landing gear performance by causing a tracking error.

In this study, SMC was applied as a control method to maintain the optimal controller performance in the presence of landing gear parameter and landing environment uncertainties and sensor noise. The SMC was applied to the hybrid control method, which resulted in the best performance among the existing controllers in terms of specific design conditions, thereby demonstrating that a stable controller performance can be maintained under various landing conditions and sensor noise. A comparison with the existing hybrid control method was performed through numerical simulation. For evaluating performance indices, the maximum compression stroke distance, maximum damper force, and impact absorption efficiency of the MR damper at landing were used. The performance was compared according to the sensor noise intensity while changing the falling speed, damping coefficient of the damper, and air chamber pressure inside the damper according to temperature for landing conditions.

This paper is organized as follows. Section 2 describes the dynamic model of a landing gear equipped with an MR damper. Section 3 details the effects of uncertainty and disturbance on the performance degradation of the hybrid control method, describes the derivation of SMC based on the Lyapunov stability theory to overcome the performance degradation, and provides the control rules of the MR damper applying SMC. Finally, Section 4 verifies the effect of the SMC based on comparison with simulation results of Simscape and Simulink.

2. Landing Gear Modeling

The landing gear equipped with an MR damper is composed of an upper chamber, a lower chamber, an air chamber, an orifice, a coil, bearing, and relief valve, as shown in Fig. 1. The impact absorption principle is the same as that of a hydraulic shock absorber.

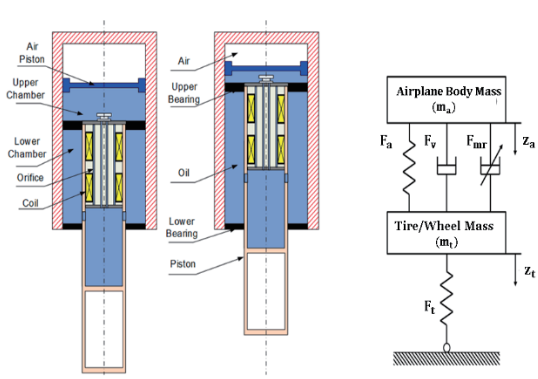

Fig. 1 Structure and FBD of an MR landing gear

2.1 Force acting on landing gear

The force acting between the upper cylinder and lower piston of the MR damper, F_d, is composed of an air force F_a, a damping force F_h, and a frictional force F_f, expressed as follows:

$$F_d = F_a + F_h + F_f. \tag{1}$$

When the landing gear touches the ground, the damper shrinks and the piston moves into the cylinder, and the air in the air chamber undergoes polytropic compression. Hence, the air force F_a can be expressed as follows:

$$F_a = A_p\left[P_0\left[\frac{V_0}{V_0 - A_p s}\right]^n - P_{ATM}\right], \tag{2}$$

where A_p is the piston cross-sectional area, P_0 is the initial pressure of the air chamber, V_0 is the initial volume of the air chamber, n is the polytropic index, and P_{ATM} is the atmospheric pressure. $s = z_1 - z_2$ is the moving distance, or the stroke of the piston from the cylinder, i.e., the difference between the sprung mass z_1 and unsprung mass z_2. The damping force F_h comprises a damping force F_v generated by the MR fluid that passes through the orifice and an additional damping force F_{MR} due to the yield stress generated by magnetic force; it can be expressed as follows [5]:

$$F_h = F_v + F_{MR}\, sgn(\dot{s}) = C\dot{s} + F_{MR} sgn(\dot{s}), \tag{3}$$

where C is the damping coefficient of the MR fluid with no current applied. The sign of F_{MR} is determined by the stroke speed $\dot{s}$.

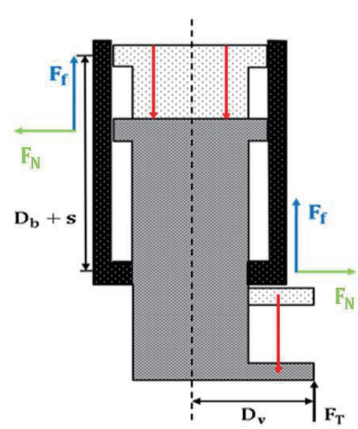

Fig. 2 Bearing Friction

The frictional force F_f between the cylinder and piston is generated from the vertical drag F_N of the bearing resulting from the distance D_v between the central axes of the tire and piston, as shown in Fig. 2. The load acting on the bearing is generated by the tilting of the piston, and because the piston is a rigid body, the sizes of the load acting on each bearing are identical. The frictional force obtained through the moment equilibrium equation with each bearing as the benchmark is as follows [11]:

$$F_f = sgn(\dot{s})\mu\frac{D_v F_T}{D_b + s}, \tag{4}$$

where μ is the dry friction coefficient, D_v the separation distance between the central axes of the tire and piston, and D_b the bearing separation when fully extended. The reaction force by the tire compression F_T is determined by the unsprung mass:

$$F_T = kz_2{}^n, \tag{5}$$

where k is the tire stiffness and n is the nonlinear index.

2.2 Equation of motion

The behavior of the landing gear during the landing of the aircraft can be categorized into two steps. The first step is the process until the aircraft touches the ground, which can be analyzed using a one-degree-of-freedom (DOF) model because the landing gear does not generate a stroke.

The second step is the process after the aircraft touches the ground, which can be analyzed by a two-DOF model because the landing gear generates a stroke.

$$\ddot{z}_1 = \frac{Am_1 g - F_d}{m_1} \tag{6}$$

$$\ddot{z}_2 = \frac{Am_2 g - F_d - F_T}{m_2} \tag{7}$$

$$z_1(0) = z_2(0) = 0 \tag{8}$$

$$\dot{z}_1(0) = \dot{z}_2(0) = v_0 \tag{9}$$

A is the remaining ratio of the aircraft gravity after an offset by the lift force. Because the impact by gravity in this study acts as a load on the landing gear, the minimum lift force becomes the harshest landing condition. Hence, A = 1 was assumed in the second step.

3. Control Method

3.1 Hybrid control method

The most important role of a landing gear is to absorb the maximum impact in a landing situation. The hybrid control method achieves the maximum landing impact absorption efficiency by maintaining a constant force between the first and second peaks in the force–displacement curve of the damper, as shown in Fig. 3. It is a combination of the Skyhook control and load control methods (see Fig. 4).

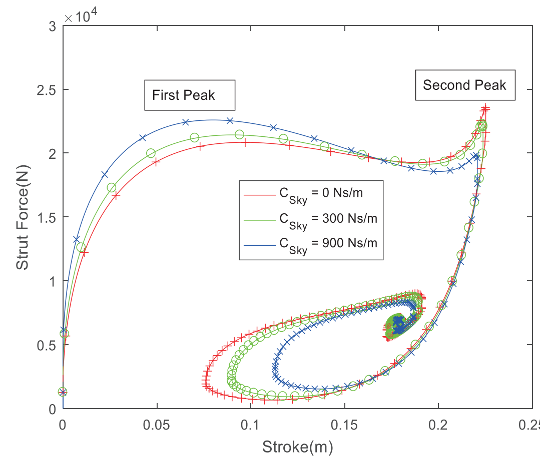

Fig. 3 Force–Displacement Curve with C_{sky}

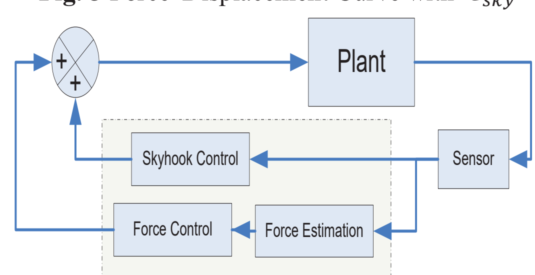

Fig. 4 Hybrid Control Diagram

The Skyhook control method is based on minimizing the motion of the sprung mass by setting a virtual damper above it; furthermore, it is the most general suspension control method. In a semi-active landing gear, only the size of the damping force can be controlled, and the direction of the damping force is determined by the stroke speed and direction. Hence, the Skyhook control input applied to the damper as the MR damping force must be calculated using the following equation [12]:

$$F_{MR} = \begin{cases} C_{sky}\dot{z}_1 & if\ \dot{z}_1\dot{s} \geq 0 \\ 0 & if\ \dot{z}_1\dot{s} < 0 \end{cases}, \tag{10}$$

where C_{sky} is the control gain obtained through trial and error.

Meanwhile, the area below the force–displacement curve in Fig. 3 is the total work of the damper. The landing impact absorption efficiency can be expressed as follows:

$$\eta(\%) = \frac{\int_{s_0}^{s_f} F_s ds}{F_{max} s_{max}} \times 100(\%) \tag{11}$$

The numerator in Eq. (11) is the total work of the damper from the initial stroke s_0 to the final stroke s_f. The denominator is the product of the maximum force F_{max} and the maximum stroke s_{max}, which occurs in the landing process and represents the area of the rectangle surrounding the force–displacement curve in Fig. 3. Therefore, the landing impact absorption efficiency η indicates the amount of curve area that fills the rectangular area, where a higher value implies more load absorption during landing.

Table 1 Performance of MR damper with C_{sky}

C_{sky} (Ns/m)	η (%)	F_{max} (kN)	s_{max} (m)
0	**83.7**	**23.6**	**0.2255**
100	**85.5**	**23.1**	**0.2250**
200	**86.3**	**22.6**	**0.2246**
300	**89.2**	**22.2**	**0.2241**
400	**90.1**	**21.7**	**0.2236**
420	**90.4**	**21.7**	**0.2235**
500	**90.2**	**21.8**	**0.2231**
600	**89.0**	**22.0**	**0.2226**

Table 1 shows the performance of the landing gear according to C_{max}. As C_{max} increases, the maximum stroke s_{max} decreases and the feeling of boarding improved. However, beyond $C_{sky} = 500\ N/s$, the maximum force F_{max} increases, thereby decreasing the landing impact absorption efficiency η. The optimal control gain must be a value where both s_{max} and F_{max} are low and η is the highest. In the force–displacement curve at this time, the force of the first peak F_{1st} becomes the same as that of the second peak F_{2nd}.

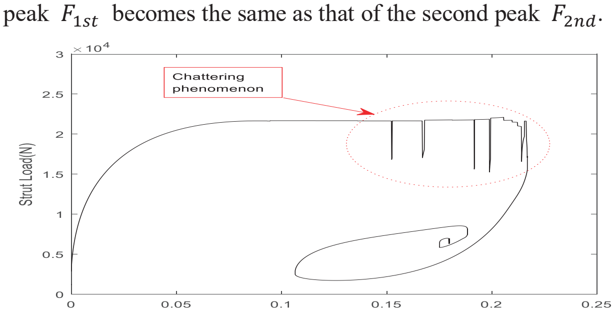

(a) Under sensor noise

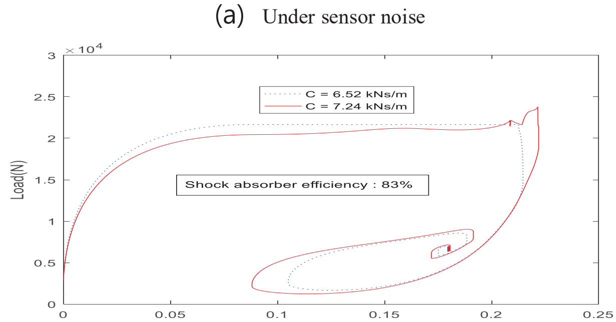

(b) Change in damping viscous coefficient

Fig. 5 Absorb efficiency under uncertainties

In the hybrid control method, the control gain value from the Skyhook control method is selected, and the force between the two peaks becomes a constant, i.e., F_{max} through the load control method when the two peak values of the force–displacement curve are identical. This can be achieved by maintaining the total damper force at F_{max} by adjusting the control input F_{MR} while setting the first peak force F_{1st} to F_{max}. To calculate the input of this hybrid control method, information regarding the stroke, speed, and acceleration of the stroke $(s, \dot{s}, \ddot{s})$ among the state variables of the damper system is required. Here, the uncertainty of the system parameters or the existence of sensor noise causes an error in the force F_d estimated according to the system state variable. This can cause a chattering phenomenon, as shown in Fig. 5, and decrease the landing impact absorption efficiency by mismatched F_{1st} and F_{2nd}.

3.2 SMC

SMC is a representative control method that addresses uncertainty. The role of SMC is to maintain the behavior of the landing gear such that it will be identical to the ideal model. The control flowchart of SMC is shown in Fig. 6.

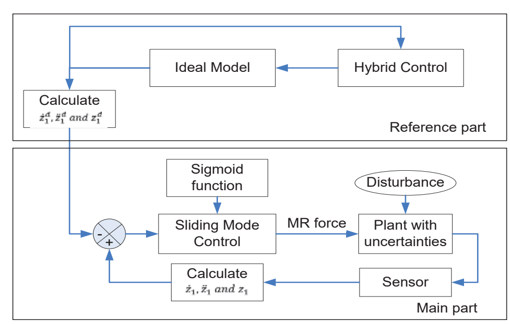

Fig. 6 Sliding Mode Control

To apply SMC, an ideal landing gear model is configured by assuming a standard landing environment and standard parameters, and the hybrid control method is applied in the method explained in the previous section. In this case, a tracking error $\tilde{z}_1 = z_1 - {z_1}^d$ is generated between the sprung mass measurement z_1 obtained from a sensor and the output of the ideal model ${z_1}^d$. The SMC used in this study was designed such that this tracking error would converge to 0. First, if the controllable damping force F_{MR} divided by the sprung mass is defined as the control input of the SMC, i.e., $u = F_{MR}/m_1$, then the equation of motion of the sprung mass (6) can be rewritten as follows:

$$\ddot{z}_1 = g - \frac{F}{m_1} - u, \tag{12}$$

where F is the sum of forces other than F_{MR}. The calculation of the damper force contains a significant error from the actual damper force because it depends on assumptions regarding the model and parameters compared with the displacement of speed measurements. Therefore, the SMC was designed to be robust to this estimation error of the damper force.

To reduce the chattering phenomenon, the following third-order integral notation was adopted for the sliding plane s_f that the state variable of the system should satisfy ($n = 3$):

$$S_f(t) = (\frac{d}{dt} + \lambda)^{n-1} \int_0^f \tilde{z}_1 dr = \dot{\tilde{z}}_1 + 2\lambda\tilde{z}_1 + \lambda^2 \int_0^f \tilde{z}_1 dr \quad (13)$$

$$\dot{S}_f(t) = \ddot{\tilde{z}}_1 + 2\lambda\dot{\tilde{z}}_1 + \lambda^2\tilde{z}_1, \quad (14)$$

where λ is the control gain, which is a positive number. Hence, $\dot{S}_f(t) = 0$ if the system state variable is maintained on the sliding plane $S_f = 0$. Furthermore, Eq. (14) shows that the sprung mass tracking error converges to zero.

Next, to obtain the control input required for the system to converge to the sliding plane, the Lyapunov candidate function V was set as show in Eq. (15), which is always positive except when $S_f = 0$.

$$V = 0.5{S_f}^2 \geq 0 \quad (15)$$

The other condition for converging to $S_f(t) = 0$ and $\dot{S}_f(t) = 0$ is $\dot{V} \leq 0$, which can be expressed as follows using Eq. (14) [13]:

$$\dot{V} = \dot{S}_f(t)S_f(t) \leq 0 \quad (16)$$

$$(\ddot{\tilde{z}}_1 + 2\lambda\dot{\tilde{z}}_1 + \lambda^2\tilde{z}_1)S_f(t) \leq 0 \quad (17)$$

$$(\ddot{z}_1 - \ddot{z_1}^d + 2\lambda\dot{\tilde{z}}_1 + \lambda^2\tilde{z}_1)S_f(t) \leq 0 \quad (18)$$

In this landing gear model, the control input $\hat{u}$ for maintaining the system on the sliding plane S_f can be calculated as follows:

$$\dot{S}_f(t) = g - \frac{\hat{F}}{m_1} - \hat{u} - \widehat{\ddot{z_1}^d} + 2\lambda\dot{\tilde{z}}_1 + \lambda^2\tilde{z}_1 = 0 \quad (19)$$

$$\hat{u} = g - \frac{\hat{F}}{m_1} - \widehat{\ddot{z_1}^d} + 2\lambda\dot{\tilde{z}}_1 + \lambda^2\tilde{z}_1 \quad (20)$$

However, the state variable disappears from the sliding plane S_f because of a tracking error from the actual system. To return to the plane, it must satisfy Eq. (16). Therefore, the control input u can be calculated as follows:

$$u = \hat{u} + \frac{k}{m_1} sgn(S), \quad (21)$$

where the constant k must be larger than the maximum estimated error of the damper force.

$$k \geq |\hat{F} - F| \quad \forall \hat{F} - F \quad (22)$$

When Eq. (21) is substituted in Eq. (18) and rearranged, we obtain

$$S_f(t)\frac{\hat{F}-F}{m_1} - |S_f(t)|\frac{k}{m_1} \leq 0 \quad (23)$$

The system converges to $S_f = 0$ because Eq. (22) is always true for any k that satisfies Eq. (23), and the sprung mass tracking error converges to 0 by Eq. (14). To prevent the chattering phenomenon, the sign function $\mathrm{sgn}(S_f)$ of the control input can be changed to the saturation function $\mathrm{sat}(S_f/\xi)$ according to the boundary layer thickness $\xi(\xi = 1)$ of the sliding plane.

Finally, the control input u of the third-order integral SMC is applied to the system as an MR damping force. As with the Skyhook control input of Eq. (10), it is determined in accordance with the following control input condition of the semi-active landing gear:

$$u = \begin{cases} \hat{u} - \frac{k}{m_1} sat\left(\frac{S_f}{\xi}\right) & if \;\; u\dot{s} \geq 0 \\ 0 & if \;\; u\dot{s} < 0 \end{cases} \quad (24)$$

4. Simulation Result and Discussion

To demonstrate the control performance of the SMC, we compared the case of applying SMC to the hybrid control method, which shows the best performance among the existing control methods, and the case of not applying SMC under specific design conditions. The simulation was performed using Simscape and Simulink simultaneously. The variables considered to simulate various landing conditions were the falling speed, damping coefficient, ambient temperature, and sensor noise. The parameters of the landing gear model and controller used in this numerical simulation are listed in Table 2.

Table 2 Parameter Data

Symbol	Quantity	Value	Unit
P_0	**Initial pressure of air chamber**	**1100**	kPa
V_0	**Initial volume of air chamber**	**6.37e-4**	m^3
A_p	**Area of head piston**	**1.3e-3**	m^2
P_{ATM}	**Atmospheric pressure**	**100**	kPa
μ	**Coefficient of friction**	**0.1**	
m_1	**Sprung mass**	**680**	kg

m_2	Unsprung mass	18	kg
n	Polytropic index	1.3	
D_v	offset between tire and piston	0.3	m
D_b	bearing separation when fully extended	0.3	m
λ	Slope of sliding surface	100	
ξ	Boundary thickness	1	
C_{sky}	Skyhook gain	420	Ns/m

The simulation results by varying the falling speeds are outlined in Table 3.

Table 3 Performance by Varying v

Hybrid Control				Hybrid Control + SMC			
v (m/s)	η (%)	s_{max} (m)	F_{max} (kN)	v (m/s)	η (%)	s_{max} (m)	F_{max} (N)
2	94.2	0.180	15.6	2	92.9	0.185	15.7
2.5	94.1	0.195	18.6	2.5	94.3	0.195	18.7
3	95.4	0.215	21.7	3	95.2	0.208	22.2
3.5	89.4	0.228	26.4	3.5	93.6	0.226	26.4

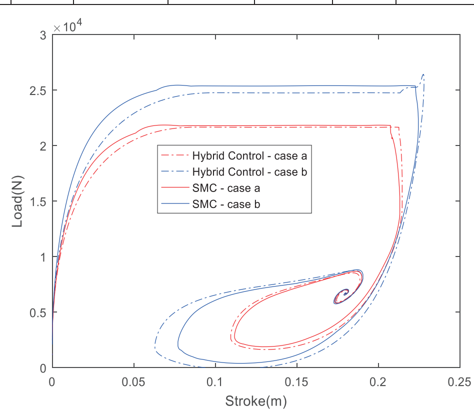

Fig. 7 Comparison Between Hybrid Control and SMC
Case a: m1 = 680 kg, v = 3 m/s.
Case b: m1 = 680 kg, v = 3.5 m/s.

The simulation results by varying the damping coefficient are outlined in Table 4.

Hybrid Control				Hybrid Control + SMC			
C (kNs/m)	η (%)	s_{max} (m)	F_{max} (kN)	C (kNs/m)	η (%)	s_{max} (m)	F_{max} (kN)
6.52	84.5	0.222	23.8	6.52	90.0	0.217	22.8
6.66	87.2	0.222	23.1	6.66	92.3	0.211	22.8
6.95	91.3	0.219	21.9	6.95	93.6	0.210	22.4
7.24	95.4	0.215	21.7	7.24	95.2	0.208	22.2

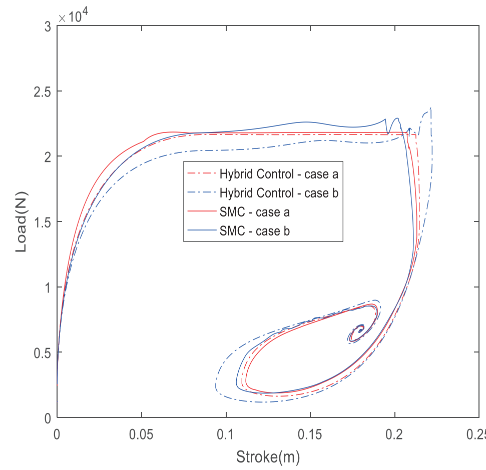

Fig. 8 Comparison Between Hybrid Control and SMC
Case a: C = 7.24 kNm/s
Case b: C = 6.5 kNm/s

The initial force of the MR damper changes according to the ambient temperature. Based on the relationship between temperature and pressure as shown in Eq. (26), the internal pressure according to temperature can be applied, as shown in Table 5.

$$\frac{P}{T} = const \tag{26}$$

T (°C)	P (MPa)
-10	8.98
0	9.3
10	9.6
20	10.0
40	10.7
50	11.0

The simulation results according to the ambient temperature are outlined in Table 6.

Hybrid Control				Hybrid Control + SMC			
T (°C)	η (%)	s_{max} (m)	F_{max} (kN)	T (°C)	η (%)	s_{max} (m)	F_{max} (N)
-10	93.4	0.224	21.1	-10	94.6	0.211	22.2
0	93.5	0.223	21.3	0	94.8	0.210	22.2
20	95.4	0.215	21.7	20	95.2	0.208	22.2

50	**93.4**	**0.208**	**23.0**	**50**	**94.9**	**0.206**	**22.4**

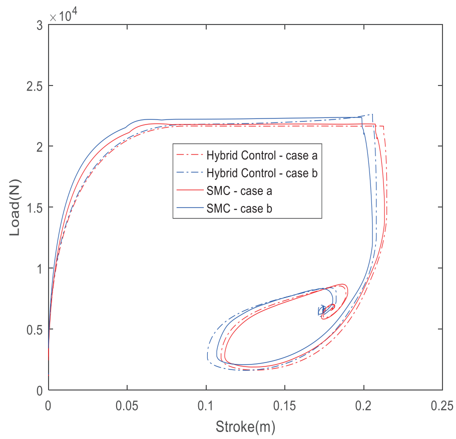

Fig. 9 Comparison Between Hybrid Control and SMC

Case a: T = 20 °C

Case b: T = 50 °C

Assuming that the error of the damper force due to the uncertainty of the damper model and the sensor data was less than 10%, the simulation results of the SMC controller using a k satisfying Eq. (26) and the existing hybrid control method are as shown in Table 7.

Hybrid Control				**Hybrid Control + SMC**			
Sensor Noise	**η (%)**	s_{max} **(m)**	F_{max} **(kN)**	**Sensor Noise**	**η (%)**	s_{max} **(m)**	F_{max} **(N)**
1%	**92.4**	**0.216**	**21.8**	**1%**	**94.4**	**0.208**	**22.2**
5%	**89.2**	**0.219**	**22.7**	**5%**	**93.0**	**0.209**	**22.5**
10%	**87.6**	**0.219**	**23.1**	**10%**	**91.7**	**0.209**	**22.6**

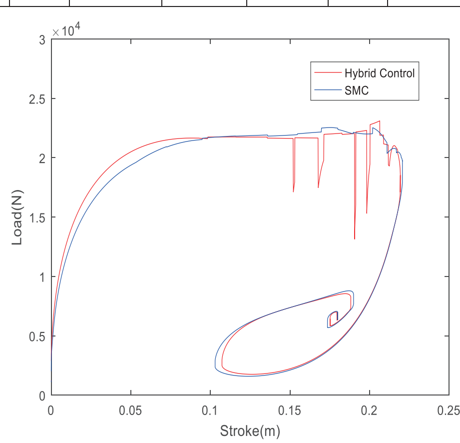

Fig. 10 Comparison Between Hybrid Control and SMC

Case: when sensor noise is present

As shown, in all the three cases where the parameters were changed, the landing impact absorption efficiency decreased except in the baseline situation, where only the hybrid control method was applied ($v = \frac{3m}{s}, C = 7.24\frac{kNs}{m}, T = 20$ ℃). However, when the hybrid control method and SMC were applied simultaneously, a high landing impact absorption efficiency and low s_{max} and F_{max} were observed even when the parameter values differed from the baseline values. In the case with sensor noise, chattering, which was generated by noise when only the hybrid control method was applied, improved considerably when it was applied together with SMC. This was because, when the system state variable disappeared from the sliding plane S_f because of the tracking error, the control input u applied a force such that the state variable returned to the sliding plane S_f by the arrival condition equation, thereby minimizing performance degradation due to errors.

5. Conclusion

Various uncertainties and sensor noise that occur in a landing situation can degrade the controller performance by generating a tracking error in the system state variable. Although many attempts have been made to solve this problem, sensor noise was not considered. In this study, the third-order integral SMC that can maintain the optimal controller performance when the landing gear has uncertainties was investigated. The existing controller applying SMC uses the hybrid control method, which combines the Skyhook control and load control methods. Four uncertainties in the landing environment were considered: variations in the falling speed, damping coefficient, ambient temperature, and sensor noise. When only the hybrid control method was applied, the landing impact absorption efficiency decreased sharply when the parameters deviated from the baseline values. This was a result of the tracking error due to the difference between the parameters of the ideal model for calculating the force and the parameters measured by the sensor. However, the control input applied through the third-order integral SMC removed the tracking error. Therefore, in a situation with uncertainties, the application of the third-order integral SMC yielded a higher landing impact absorption efficiency and lower s_{max} and F_{max} compared with those of the hybrid control method. This suggests that the third-order integral SMC provided robustness against uncertainties in the system.

Acknowledgement

This work was conducted under the support of the Korea Evaluation Institute of Industrial Technology as part of the "Aerospace Parts Technology Development Project (10073291)" of the Ministry of Trade, Industry, and Energy. We would like to express our sincere gratitude for this support.

References

[1] N. S. Currey, “Aircraft Landing Gear Design: Principle and Practices”, *American Institute of Aeronautics and Astronautics*, Washington, D.C., pp. 69-121, 1988.

[2] J. R. McGehee and H. D. Carden, “A mathematical model of an active control landing gear for load control during impact and roll out”, *NASA Langley Research Center*, Hampton, Va. 23665, Rep. NASA TND -8080, February 1976.

[3] G. L. Ghiringhelli, “Testing of semi-active landing gear control for a general aviation aircraft”, *Journal of Aircraft*, vol. 37, no. 4, pp. 606-616, July-August 2000.

[4] Y. O. Hyun, “Semi-active hybrid control method of landing gear using magneto-rheological damper”, Ph.D. Thesis, *Korea Aerospace University*, Gyeong-gi, Republic of Korea, 2009.

[5] C. Han, B. –G. Kim, and S. –B. Choi. “Design of a new magnetorheological damper based on passive oleo-pneumatic landing gear”, *Journal of Aircraft*, pp. 2510-2520, 2018.

[6] J. M. Tak et al., “Hybrid control of aircraft landing gear using magnetorheological”, *Journal of Aerospace System Engineering*, vol. 12, no. 1, pp. 1-9, 2018.

[7] G. Mikulowski, “Adaptive aircraft shock absorbers”, *AMAS Workshop on Smart Materials and Structures*, *SMART’03*, pp. 63-72, September 2003.

[8] X. M. Dong and G. W. Xiong, “Vibration attenuation of magnetorheological landing gear system with human simulated intelligent control”, *Journal of Mathematical Problems in Engineering*, vol. 2013, 2013.

[9] A. A. Gharapurkar, “Robust semi-active control of aircraft landing gear system equipped with magnetorheological dampers”, M.S. Thesis, *Department of Mechanical Engineering, Concordia University*, Montreal, Quebec Canada, 2014.

[10] Y. T. Choi and N. M. Wereley, “Vibration control of a landing gear system featuring electrorheological/ magnetorheological fluids”, *Journal of Aircraft*, vol. 40, no. 3, pp. 432-439, May-June 2003.

[11] B. Milwitzky and F. E. Cook, “Analysis of landing – gear behavior”, Langley Aeronautical Laboratory Langley Field, Rep. 1154, May 1948.

[12] S. B. Choi and Y. M. Han, “Fluid technology applications in vehicle systems”, *CRC Press Taylor & Francis Group*, pp. 2-11, 2013.

[13] J. J. E. Slotine and W. Li, “Applied nonlinear control”, *Prentice Hall International.*